THE JOURNAL OF COMPARATIVE NEUROLOGY 419:306–319 (2000)

Termination of the Geniculocortical Projection in the Striate Cortex of Macaque Monkey: A Quantitative Immunoelectron Microscopic Study

DIANE LATAWIEC,* KEVAN A.C. MARTIN, AND VIRGINIA MESKENAITE
Institute of Neuroinformatics, University/ETH Zurich, CH-8057, Zürich, Switzerland

ABSTRACT

The goal of this present study was to derive a new estimate of the synaptic contribution of the dorsal lateral geniculate nucleus (dLGN) to the subdivisions of its main recipient layer, layer 4C, of striate cortex of macaque monkey. The projection from the dLGN and its terminal boutons within layer 4C were visualized by immunodetection of the calcium binding protein, parvalbumin (PV), which is expressed in relay cells of the dLGN. The proportion of asymmetric synapses formed by PV-positive boutons within the α and β sublayers of 4C was estimated by using a nonbiased stereological counting method. The proportion of asymmetric synapses contributed by the PV-positive boutons to layer 4Cα is 8.7%; to 4Cβ is 6.9%. Assuming all the PV-positive asymmetric synapses derive from the dLGN relay cells, this gives a ratio of dLGN synapses per neuron of 192 in layer 4Cα and 128 in layer 4Cβ. Thus, the recurrent excitatory input from neighboring cortical neurons must play an important part in responses of the neurons lying at the input stage of the cortical circuit. J. Comp. Neurol. 419:306–319, 2000.

Indexing terms: visual cortex; dorsal lateral geniculate nucleus; layer 4C; parvalbumin; physical disector method

Physiological studies in the monkey primate visual cortex have shown that most neurons in the main thalamorecipient layer, (layer 4C) are not only the "simple" type found in layer 4 of the cat, but may resemble more those of the dorsal lateral geniculate (dLGN) neurons, particularly in layer 4Cβ (Hubel and Wiesel, 1968; Blasdel and Fitzpatrick, 1984; Hawken and Parker, 1984; Livingstone and Hubel, 1984). However, some simple and complex cells are found mixed with nonorientated cells in layer 4C (Blasdel and Fitzpatrick, 1984; Hawken and Parker, 1984; Leventhal et al., 1995). The reasons for this very marked difference between cat and monkey are unknown, but differences in the convergence of the dLGN afferents may be a contributing factor. In the cat, it is estimated that about 300 of the 5,000 excitatory synapses formed with each layer 4 neuron originate from the dLGN (Peters and Payne, 1993; Ahmed et al., 1997). In the monkey, Peters et al. (1994) have estimated that only 18–40 synapses per layer 4Cα neuron originate from the magnocellular layers of the dLGN, and between 37 and 191 synapses per layer 4Cβ neuron originate from the parvicellular layers of the dLGN. These remarkably low numbers correspond to a contribution from the dLGN of less than 2% of synapses in layer 4Cα and 4–9% of the synapses in layer 4Cβ.

The estimates by Peters et al. (1994) were derived by calculation from a diverse collection of data. Unfortunately, direct studies in the monkey are rare. Garey and Powell (1971) used degeneration methods to determine that between 5% and 10% of the synapses in layer 4C of the macaque monkey originate from the dLGN. Their sampling and counting methods and data were not reported. The New World monkey has provided yet other numbers. Tigges and Tigges (1979) reported that on average 16–19% of the boutons in layer 4 of the squirrel monkey degenerated after making a lesion in the dLGN,

Grant sponsor: SNSF; Grant number: 5002-044888.

*Correspondence to: Diane Latawiec, Institute of Neuroinformatics, University/ETH Zurich, Winterthurerstrasse 190, CH-8057, Zürich, Switzerland. E-mail: diane@ini.phys.ethz.ch

Received 2 September 1999; Revised 2 November 1999; Accepted 9 December 1999

but that individual patches could show as high as 29%, which they thought was closer to the "real" number.

DeFelipe and Jones (1991) studied the mode of termination of the dLGN afferents in layer 4Cβ by exploiting the fact that the relay neurons in the dLGN of the macaque monkey contain the calcium-binding protein, parvalbumin (PV; Jones and Hendry, 1989). They discovered that the thalamic terminals concentrated in "microzones" of 10–50 μm diameter, in which thalamic synapses formed about 32% of the asymmetric synapses. Outside the microzones, the thalamic synapses contributed 9% of asymmetric synapses. Their "preliminary quantitative analysis" of the density of the microzones was that there were 3–8 microzones per 10,000 μm^2 and that the patches were 10×20 μm^2 in size, i.e., the microzones occupy ~11% of layer 4Cβ. On the basis of these numbers, we calculate that the higher density of PV in the microzones contributes to an overall mean proportion of dLGN synapses in layer 4Cβ of 10.4% of asymmetric synapses. The equivalent numbers for 4Cα were not given (DeFelipe and Jones, 1991).

An accurate determination of the proportion of dLGN synapses in the monkey is important for a number of reasons. We need to discover whether the physiological differences in layer 4 receptive fields between cat and monkey is related to the proportion of dLGN synapses that single cells receive. In the monkey, single dLGN afferents might provide more of the excitatory drive to single neurons in layer 4 (Blasdel and Lund, 1983; Blasdel and Fitzpatrick, 1984) so that the receptive field would resemble more those of individual dLGN neurons. Against this possibility, Peters et al. (1994) estimated that the 4Cα cells receive a much smaller input from the dLGN than the 4Cβ cells. We need to find out whether the geniculocortical projection in the monkey is quantitatively different from the cat. If the percentage of dLGN synapses formed on any neuron is high, then the dLGN should dominate the responses of the neurons. Alternatively, a low proportion of dLGN synapses in the monkey would also indicate that other sources of excitatory synapses must contribute significantly to the responses of layer 4 cells.

For these reasons, we have made a new electron microscopic study of the geniculocortical projection to layer 4C in the macaque monkey. Instead of using the conventional methods of degeneration or anterograde tracers, we exploited the fact that the dLGN relay cells appear to be the principal source of parvalbumin-positive (PV+) boutons that form asymmetric synapses in layer 4C (Jones and Hendry, 1989; DeFelipe and Jones, 1991). This meant that the geniculocortical projection could be identified directly in normal rather than experimental material obtained from conventional tracing methods. Our results indicated that about 8% of the asymmetric synapses in layer 4C were formed by PV+ boutons. This percentage translates to a convergence of dLGN synapses per layer 4 neuron for both 4Cα and 4Cβ that is comparable to the value found in the cat.

MATERIALS AND METHODS

Tissue preparation

Material was obtained from six adult macaque monkeys (*Macaca fascicularis*) that had been used in prior physiological experiments, which involved single unit recording from one hemisphere. All tissue used here was taken from the opposite hemisphere. Monkeys were deeply anesthetized with a dose of Nembutal (80–100 mg/kg) and perfused transcardially, first with physiological saline, followed by a fixative made up in 0.1 M phosphate buffer (PB) pH 7.4. The fixatives used were: (1) 4% paraformaldehyde with 0.025% glutaraldehyde (one monkey), (2) 2–2.5% paraformaldehyde with 0.3–0.6% glutaraldehyde (two monkeys), (3) 4% paraformaldehyde, 0.3% glutaraldehyde, and ~ 0.2% picric acid (one monkey), or (4) 2.5% paraformaldehyde, 0.05% glutaraldehyde, and ~ 0.2% picric acid (two monkeys). The 3 monkeys perfused without picric acid in the fixative were used for the electron microscopy study of synapses within layer 4C of striate cortex. The other 3 monkeys were used in single and double immunocytochemical labeling experiments on sections of the dLGN.

Blocks of striate cortex and the dLGN were taken from the intact hemispheres of all experimental monkeys, and cut in the sagittal and frontal planes, respectively, and washed overnight in 0.1 M PB. The blocks were cryoprotected first in 10% and then 20% sucrose made up in 0.1 M PB, frozen in liquid nitrogen, and thawed in 0.1 M PB in an attempt to improve penetration of immunoreagents. Sections were cut on a vibratome (70 μm) and washed in repeated changes of 0.1 M PB (5×30 minutes). In some cases, alternate sections of striate cortex were stained for cytochrome oxidase (CO; Wong-Riley, 1979). The pattern of the cytochrome oxidase distribution was used to aid in defining the laminar borders (Fitzpatrick et al., 1985). These experiments were carried out under an animal research license granted by the Cantonal Veterinary Authority of Zürich.

Parvalbumin immunocytochemistry

Free-floating sections from both the striate cortex and the dLGN were first incubated in 20% normal goat serum (NGS) for 40 minutes at room temperature (RT), followed by a 3-day incubation at 4°C in a mouse-anti-PV antibody (SWant, Bellinzona, Switzerland; 1:20,000) diluted in 2% NGS in 0.05 M Tris-buffered saline (TBS) pH 7.4. After extensive washing in TBS (3×30 minutes), the sections were incubated overnight at 4°C in a biotinylated goat anti-mouse antibody (Vector Laboratories, Peterborough, England; 1:200) followed by a 6-hour incubation at RT in an avidin-biotin-peroxidase complex (ABC; Vector Laboratories, Peterborough, England; 1:100). Antigenic sites were visualized with standard 3-3′-diaminobenzidine tetrahydrochloride (DAB; Sigma, Buchs, Switzerland) histochemistry. Sections for light microscopy were mounted onto gelatinized slides, air-dried, dehydrated, and coverslipped in Entellan (Merck, Dietikon, Switzerland). Sections for electron microscopy were postfixed in a solution of 1% osmium tetroxide in 0.1 M. PB, contrasted with 1% uranyl acetate dissolved in 70% ethanol for 1 hour, dehydrated, and flat-embedded onto slides in Durcupan ACM resin (Fluka, Buchs, Switzerland).

CaM II kinase immunohistochemistry

In addition, free-floating sections of the dLGN were immunoreacted for the type II calmodulin-dependent protein kinase (CaM II kinase). In the macaque dLGN, this kinase has been shown to be expressed by the population of koniocellular (K) cells. The "K" cells largely occupy the

"S" and "interlaminar" layers (Hendry and Yoshioka, 1994) and project to the cytochrome oxidase puffs in layers II and III (Hendry and Yoshioka, 1994; Hendry and Calkins, 1998). Moreover, some cells are found randomly scattered throughout the principal layers or in the form of "bridges" (Hendry and Yoshioka, 1994).

After incubation of sections in 20% NGS for 40 minutes, sections were incubated for 2 days at 4°C in a mouse-anti-CaM II kinase antibody (Böehringer Mannheim, Rotkreuz, Switzerland; 1:100). A biotinylated goat-anti-mouse antibody (Vector Laboratories, Peterborough, England; 1:200) was used as the secondary link antibody before incubation of the sections for 1 ¼ hours at RT in the ABC complex. Antigenic sites were revealed with standard DAB histochemistry. Sections were postfixed in 1% osmium tetroxide, dehydrated, and flat-embedded onto slides in Durcupan ACM. The distribution of the CaM II kinase-immunoreactive cells in the dLGN were analyzed and drawn under a microscope with drawing tube attachment (Fig. 2A).

Double labeling parvalbumin/GABA immunohistochemistry

To verify whether all relay cells projecting to layer 4C were PV+, an antibody for gamma-aminobutyric acid (GABA) was used in conjunction with a PV antibody to differentiate relay cells from local circuit neurons in the dLGN. Free-floating sections of the dLGN were preincubated in 20% NGS for 40 minutes at RT, before a 3-day incubation at 4°C in a mixture of rabbit-anti-PV antibody (SWant, Bellinzona, Switzerland; 1:3,000) and rat-anti-GABA antibody (NT 103, Eugene Tech. International Inc.; 1: 250), which had been diluted in 2% NGS. After extensive washing in TBS (3 × 30 minutes), sections were incubated overnight at 4°C in a mixture of goat-anti-rabbit antibody (ICN, Basingstoke, England; 1:50) and biotinylated goat-anti-rat antibody (Vector Laboratories, Peterborough, England; 1:200). Antigenic sites for GABA were revealed after further incubation in the ABC complex (1:100) by using a method of heavy metal intensification of DAB (Hsu and Soban, 1983) which resulted in a blue/black reaction end product. Antigenic sites for PV were revealed by further incubation of sections in a rabbit anti-peroxidase complex (Dakopatts, Ely, England; 1:100) and standard DAB histochemistry, which resulted in a brown reaction end product. The sections were mounted onto gelatin-coated slides and air-dried overnight, prior to light counterstaining of sections with toluidine blue. Staining the tissue with toluidine blue served to identify and separate the unlabeled neurons and glial cells from neurons labeled immunohistochemically.

Sections from both the posterior and more central portions of the dLGN were analyzed for nonimmunolabeled somatic profiles. Vertical strips, extending from dorsal to ventral, through all layers, were taken from the central region of the sections. These covered an area of approximately 2 mm^2. On two sections, one from the posterior portion, the other more central to this, all immunolabeled somatic profiles and histochemically labeled profiles on the cut surface of the tissue lying within the strip, were drawn and analyzed at ×40 magnification on a microscope with camera lucida attachment. Any somatic profile that appeared to be nonimmunolabeled was verified with oil immersion at ×100 magnification.

Control incubations

As controls for specific immunoreactivity, sections of both the dLGN and striate cortex were incubated with the omission of the primary antibodies or secondary link antibody. Under these conditions, immunoreactivity resembling those obtained by using the specific antibodies could not be detected.

Quantification of synapses

Tissue was taken from each sublayer of layer 4C (4Cα and 4Cβ) of the striate cortex, from the opercular region of the parafoveal representation and reembedded into blocks. The sublayers were delineated according to the scheme of Fitzpatrick et al. (1985). Layer 4C was divided into two equal halves; the upper half was defined as layer 4Cα, and the lower as layer 4Cβ. Due to limited antibody penetration, serial ultrathin sections were only taken from the cut surface of the tissue to a depth of 5 μm and collected on single slot pioloform coated copper grids.

Synapses were quantified based on the physical disector method (Sterio, 1984; Gundersen, 1986; Coggeshall and Lekan, 1996; Geinisman et al., 1996). The method entails using two randomly chosen sections to make a "disector" pair. The first section is referred to as the "reference section," the second as the "look-up" section. In this study, the "look-up" section of the disector was always the second section after the reference section. Disectors were taken only in areas from the upper part of layer 4Cα and lower part of layer 4Cβ. Disectors were not taken from the middle of layer 4C to avoid any possible overlap between the sublayers. Sections were analyzed on a Philips CM 100 electron microscope and photographed at ×11,500 magnification. Only synapses that "disappeared" in the "look-up" section were identified and counted.

The numerical density of synapses (number per unit volume, Nv) was derived using the disector method, and calculated according to the formula:

$$\mathrm{Nv} = \frac{\Sigma Q\text{-}}{a \times h}$$

where Q- is the number of synapses appearing in the test area of the reference section but absent in the look-up section. The volume reference corresponds to the area sampled (a) multiplied by the disector height (h), which is the distance between the two sampling sections (Gundersen, 1986; Coggeshall, 1992). For determination of the distance between the reference and the look-up sections, the section thickness was measured by using Small's method of minimal folds (Small, 1968) as described by Weibel (1979) and Royet (1991). This method provides accurate estimates of section thickness compared with other techniques (Calverley et al., 1988; DeGroot, 1988; Hunter and Stewart, 1989). Minimal folds lie perpendicular to the section plane and have a width that equals twice that of the section thickness. Minimal folds were identified in the disectors and photographed at × 21,000 magnification. The minimal fold width was measured directly on the micrographs and the values were averaged to obtain a section thickness of 56 ± 3 nm from 30/32 disectors.

Synapses were classified independently by all three authors into one of the following three categories: (1) nonimmunoreactive (non-ir) asymmetric; (2) parvalbumin-

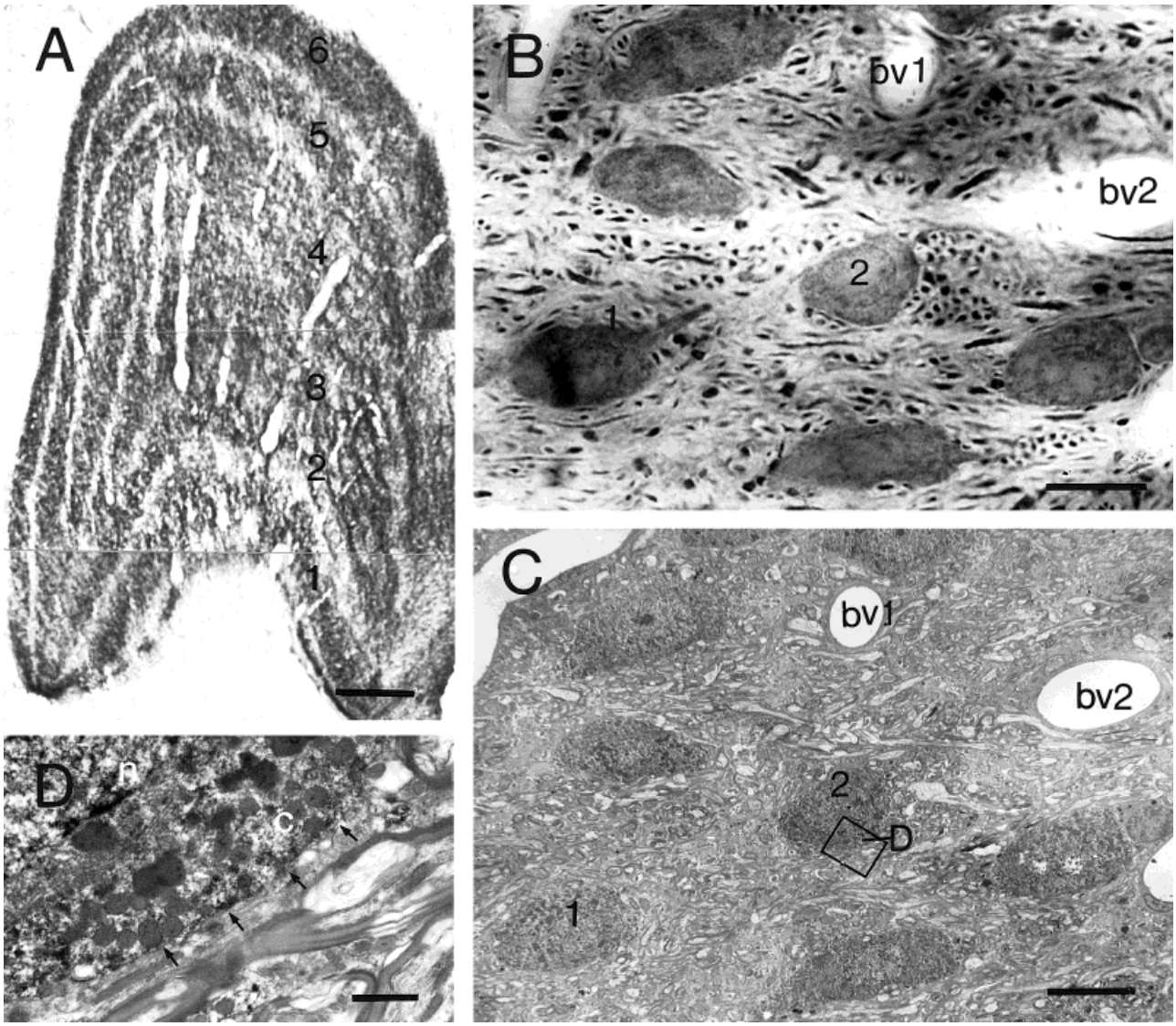

Fig. 1. Light and electron micrographs showing the immunoreactivity of parvalbumin in the dorsal lateral geniculate nucleus (dLGN) of macaque monkey. **A:** In the dLGN, parvalbumin (PV) immunoreactivity was revealed in all principal layers, 1–6. **B** and **C:** Correlated light and electron micrographs of a group of PV-immunoreactive (ir) cells from parvicellular layer 4. In B, a higher-power micrograph of PV-ir cells in osmicated material revealed PV-ir to be "variable" even between cells from the same area and section depth. In this group of cells, cell 1 was most strongly labeled, whereas cell 2 was the lightest labeled for PV. bv, blood vessel. C: A low-power electron micrograph of the same group of cells confirmed all the cells in B were PV-ir. **D:** A higher-power electron micrograph of the boxed area in cell 2, revealed the electron-dense peroxidase reaction end product (which indicates PV immunoreactivity) deposited throughout the cell cytoplasm. Arrows indicate the plasma membrane of cell 2. c, cytoplasm; n, nucleus. Scale bars = 400 μm for A; 10 μm for B, C; 1 μm for D.

immunoreactive (PV-ir) asymmetric; and (3) non-ir and PV-ir symmetric. Classification of a synapse was based on the criteria and nomenclature of Peters et al. (1990, 1991). A synapse was identified by the apposition of two profiles with a clustering of synaptic vesicles near the presynaptic membrane and either by the presence of a pronounced postsynaptic density (asymmetric) or a lack of an obvious postsynaptic density (symmetric). The presence of electron-dense peroxidase reaction end product in a presynaptic axonal bouton forming an asymmetric synapse with its postsynaptic target was assumed to identify a bouton from a dLGN afferent (Figs. 4A, 5A,B, 7A–C, filled arrows). Occasionally, classifying a synapse in a disector from the electron micrographs of the reference and look-up section proved difficult and required examination of adjacent serial sections to make the classification. However, nine synapses still could not be classified into any category and were thus excluded.

Postsynaptic targets were classified on the basis of being either PV-ir or non-ir. By using the ultrastructural criteria of Peters et al. (1990, 1991), targets were further classified into spine, dendritic shaft, or soma. Ambiguous targets were verified by examination of the serial sections adjacent to the disector sections.

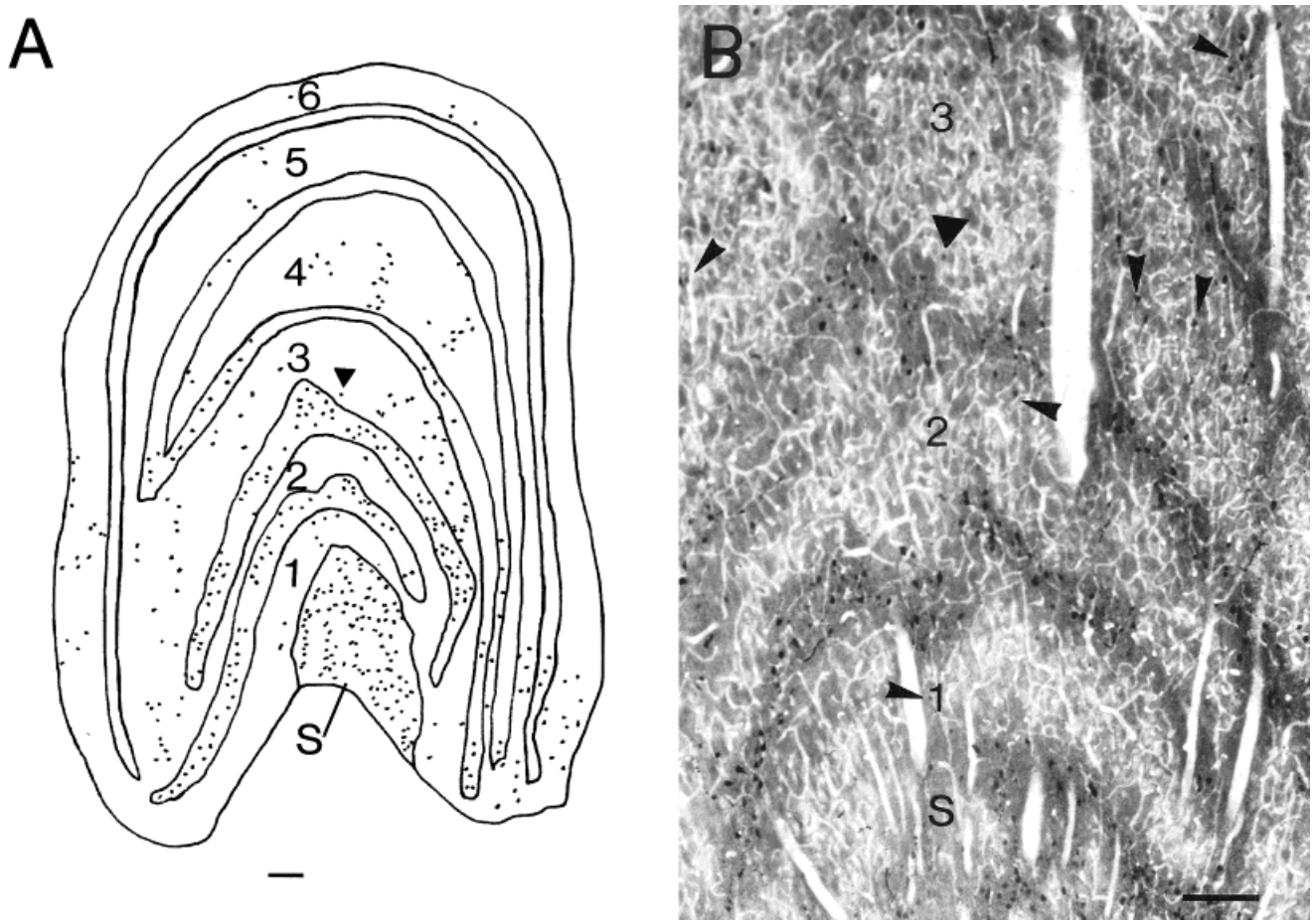

Fig. 2. A camera lucida drawing and light micrograph of a transverse section of the dorsal lateral geniculate nucleus (dLGN) of macaque monkey showing the pattern of type II calmodulin-dependent protein kinase (CaM II kinase) immunoreactivity. **A:** CaM II kinase immunoreactivity was present in all layers of the dLGN. The most intense staining was confined to the "S" layer and the "interlaminar layers"; in particular, the interlaminar layers which lie ventral to magnocellular layers 1 and 2 and parvicellular layer 3. A and **B:** In the principal layers (1–6), CaM II kinase-immunoreactive neurons were rare. Arrowheads in B indicate examples of the randomly scattered CaM II kinase-immunoreactive cell population. Triangles locate the same area of the dLGN in both A and B. Scale bars = 200 μm.

RESULTS

Dorsal lateral geniculate nucleus

In the dLGN, PV-ir clearly delineated the magnocellular (layers 1 and 2) and the parvicellular layers (layers 3–6) from the interlaminar zones (Fig. 1A). The intensity of PV-ir was consistently stronger in the parvicellular layers compared to the magnocellular layers, although within the layers themselves, PV-ir was variable (Fig. 1B). Analysis at the electron microscopy level confirmed this observation (Fig. 1C). In the interlaminar layers, PV-ir was low (Fig. 1A). As reported previously by Hendry and Yoshioka (1994) however, CaM II kinase immunoreactivity was confined mainly to the S and interlaminar layers, in particular the layers dorsal to magnocellular layers 1 and 2 (Fig. 2A). Occasional clusters of CaM II kinase-immunoreactive cells formed bridges through the width of the principal layers (Fig. 2A and B).

As DeFelipe and Jones (1991) mentioned, they could not rule out the possibility that the PV-ir thalamocortical axons may originate only from a subpopulation of the dLGN relay cells. We examined this by immunoreacting sections of dLGN for GABA and PV. This procedure labeled the dLGN interneurons, which are all GABA-immunoreactive (GABA-ir; Montero and Zempel, 1986) and all PV-ir relay cells. If there were a significant population of non–PV-ir relay cells, these would remain unlabeled. Extensive examination of 5 immunoreacted sections gave no indication that there were significant numbers of unlabeled neurons. Practically all of the neuronal profiles in the dLGN were labeled with either antibody to GABA or PV or both. Quantitative counts on 2 sections, one from the posterior portion of the dLGN and the other more central to this section (from 2 monkeys), confirmed this. Only 12 of 3,123 somata examined in the magno- and parvicellular layers were unlabeled and presumably these were the neurons of the K pathway, which do not stain for GABA or PV and which project outside layer 4C (Jones and Hendry, 1989; Hendry and Yoshioka, 1994; Hendry, personal communication). From this, we conclude that there is no

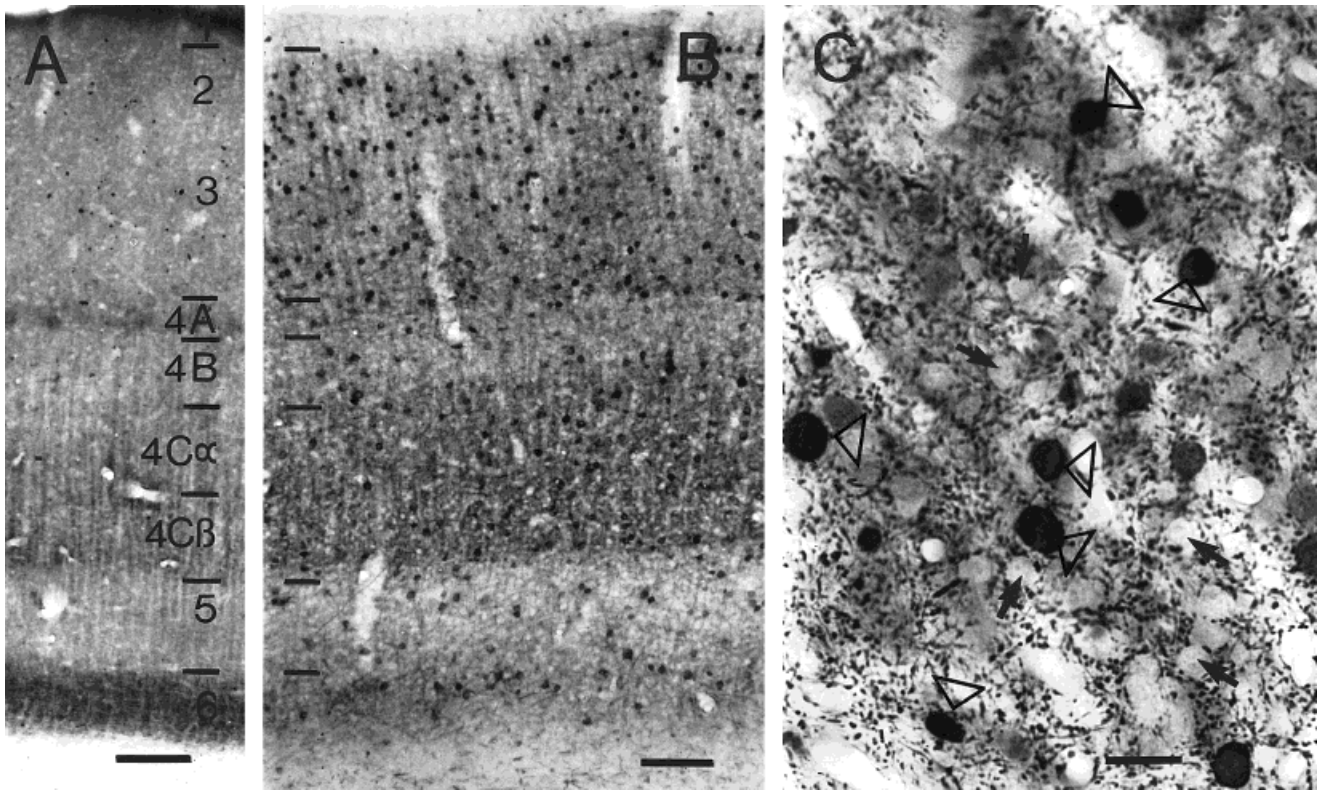

Fig. 3. Light micrographs showing the immunoreactivity of parvalbumin in area 17 of primary visual cortex in macaque monkey. **A:** Cytochrome oxidase stained sagittal section of area 17, adjacent to the parvalbumin (PV)-immunoreacted section in **B**, which reveals the laminar distribution pattern of PV immunoreactivity. Note the distribution of PV-immunopositive neurons through all layers. **C:** A high-power light micrograph of layer 4C shows PV-immunoreactive (ir) puncta densely distributed between non-ir (filled arrows) and PV-ir (open arrowheads) somata in the neuropil. Scale bars = 200 μm for A and B; 50 μm for C.

significant number of non PV-ir relay neurons in the dLGN that project to layer 4C. Additionally, after visualizing the sections firstly for PV, some neurons with small somata were also observed to label strongly for PV. On grounds of their small size, these are likely to be GABAergic neurons (Jones and Hendry, 1989).

Electron microscopy of synapses within layer 4C of striate cortex

The distribution pattern of PV-ir in striate cortex was compared with a section reacted for CO (Fig. 3A,B). The CO staining has been shown to match the location of lateral geniculate terminations in layer 4C (Blasdel and Fitzpatrick, 1984; Fitzpatrick et al., 1985) and so was used here for defining the laminar borders. Consistent with this, the distribution of PV-ir has also been shown to match the distribution patterns of CO staining in macaque monkey (Kennedy et al., 1985; Van Brederode et al., 1990; Blümcke et al., 1990). In layer 4C, PV-ir in the neuropil appeared to be nonhomogenous, but densely distributed between unlabeled (Fig. 3C, filled arrows) and PV-labeled somata (Fig. 3C, open arrowheads). No layer 6 pyramidal cells, some of which have axonal terminations in layer 4C (Lund and Boothe, 1975; Anderson et al., 1993; Wiser and Callaway, 1996), expressed PV at detectable levels.

Parvalbumin labeling of synaptic boutons in layer 4C, identified by the presence of the electron-dense peroxidase reaction end product, revealed two distinct populations, one forming asymmetric synapses and the other forming symmetric synapses (Figs. 4,5).The PV-ir boutons that formed asymmetric synapses were assumed to originate from relay neurons of the dLGN (Figs. 4A, 5A,B, 7A–C). The density of the peroxidase reaction end product appeared mainly to be higher in neurons that form symmetrical synapses regardless of the sublayer. Previous studies in macaque monkey have indicated this to be a subclass of the cortical GABAergic inhibitory neurons, i.e., the basket cell (Hendry et al., 1989; Blümcke et al., 1990; Van Brederode et al., 1990) and chandelier cell (DeFelipe et al., 1989; Lewis and Lund, 1990). By contrast, the PV-ir boutons that formed asymmetric synapses revealed that the density of the reaction end product seemed to be higher in boutons in layer 4Cβ than in layer 4Cα. (Compare boutons 1 and 2 in Fig. 5 with boutons 1 and 2 in Fig. 4.) This confirmed observations seen at the light microscopy level.

The proportion of asymmetric synapses formed by afferents of the dLGN

From the 3 monkeys, 10 disector pairs were made from one monkey, 13 from another, and 9 from the third monkey, to satisfy the requirements of the sampling method (Sterio, 1984; Coggeshall and Lekan, 1996; West, 1999). In total, 389 synapses were classified in layer 4C. In layer 4Cα, we counted 193 synapses and in 4Cβ 196 synapses.

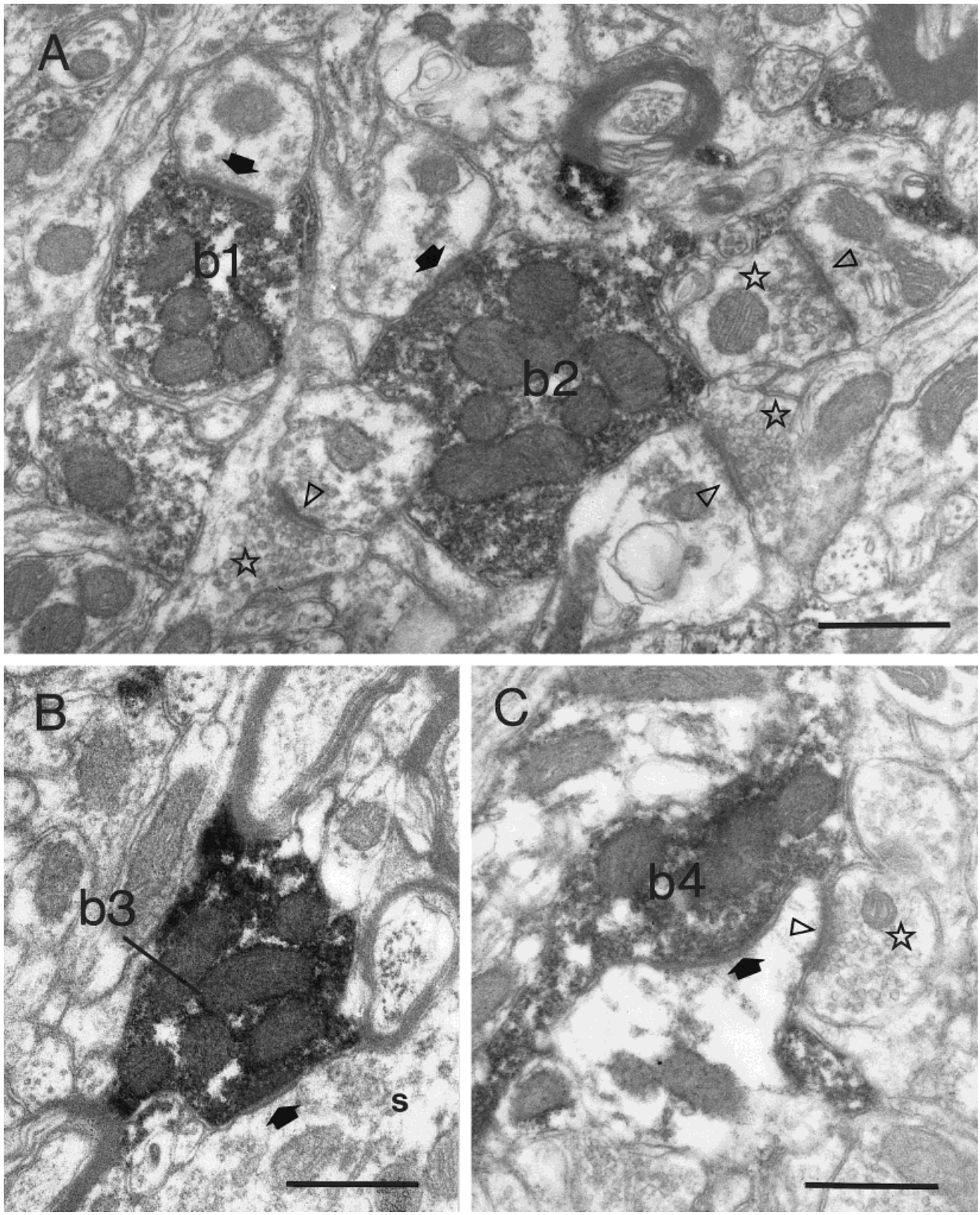

Fig. 4. Electron micrographs of synapses formed by parvalbumin-immunoreactive (PV-ir) boutons in the magno-recipient layer 4Cα of macaque monkey. **A:** Two large PV-ir boutons (b1, b2) putatively from dorsal lateral geniculate nucleus (dLGN) afferents form asymmetric synapses (filled arrows) with their non–PV-ir targets. The star identifies non-ir boutons forming asymmetric synapses (open arrowheads) with their targets. **B** and **C** shows two PV-ir boutons (b3, b4) forming symmetric synapses (filled arrows) with non-ir targets. s, soma. In C, the postsynaptic target of b4 also forms an asymmetric synapse with a non-ir bouton (star). Scale bars = 0.5 μm.

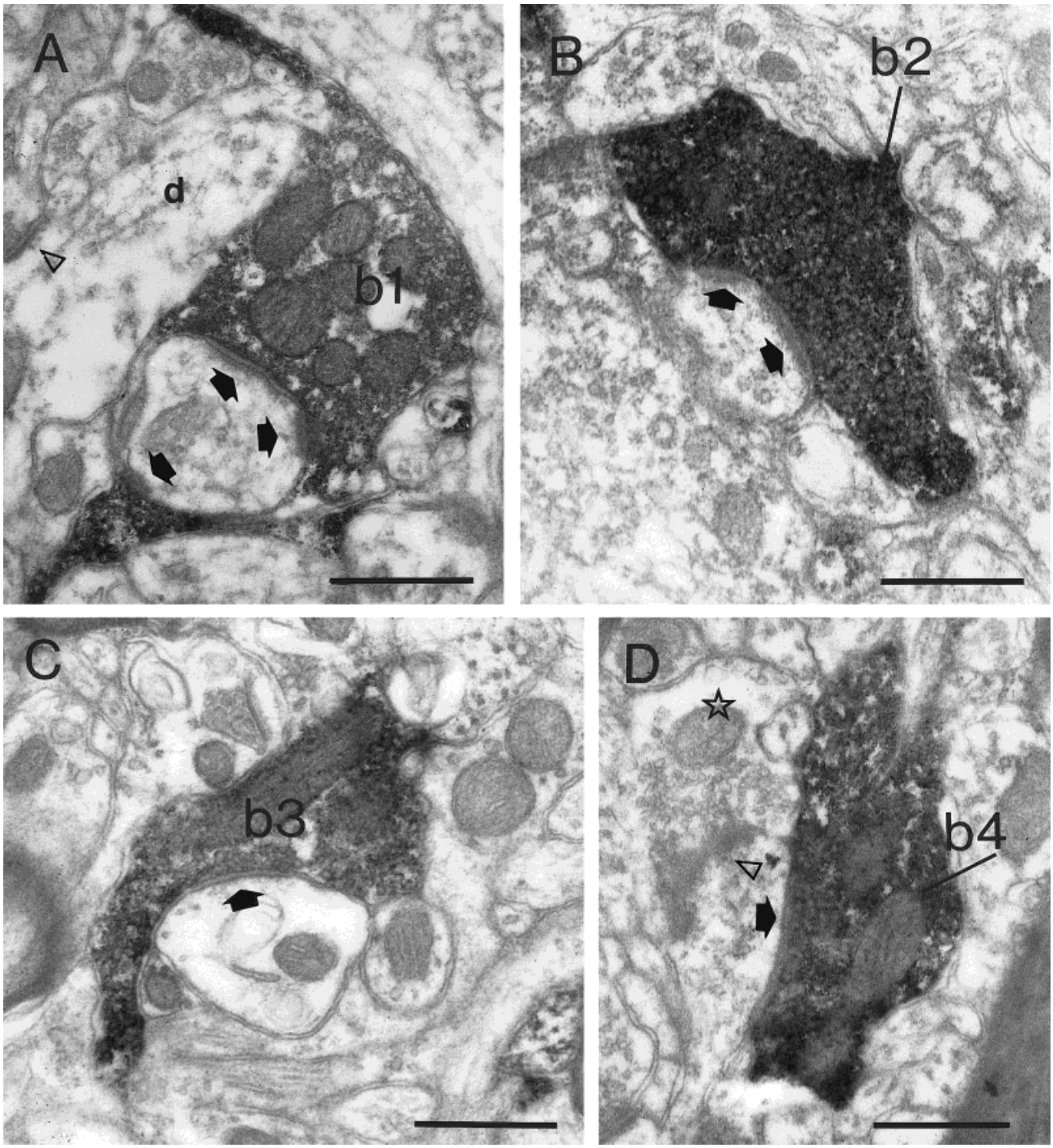

Fig. 5. Electron micrographs of synapses formed by parvalbumin-immunoreactive (PV-ir) boutons in the parvi-recipient layer 4Cβ of macaque monkey. **A** and **B** show two large PV-ir boutons (b1, b2) from putative dorsal lateral geniculate nucleus (dLGN) afferents forming asymmetric synapses (filled arrows) with their non-ir targets. Notice that b1 appears to almost totally wrap itself around its postsynaptic target. **C** and **D** show two PV-ir boutons (b3, b4) forming symmetric synapses with their postsynaptic targets (filled arrows). In addition, the postsynaptic target of b4 also forms an asymmetric synapse (cut obliquely, open arrowhead) with a non-ir bouton (star). d, dendrite. Scale bars = 0.5 μm.

The mean density of all asymmetric synapses (labeled and unlabeled) for the 3 monkeys was 183×10^6 per mm^3 (159–221) for layer 4Cα and 274×10^6 per mm^3 (219–357) for 4Cβ (uncorrected for shrinkage, ranges in brackets). For the symmetric synapses, the comparable densities and ranges were 22×10^6 per mm^3 (9–43) for layer 4Cα and 38×10^6 per mm^3 (26–55) for 4Cβ. Thus, although the absolute density of synapses varied between sublaminae,

TABLE 1. Summary From Three Monkeys of the Mean Percentage Distributions and Targets of the Synapse Categories

	Synapse category		
	Non-ir[2] asymmetric (%)	PV-ir[3] asymmetric (%)	Non-ir + PV-ir symmetric (%)
Recipient layer			
Magno-recipient layer 4Cα (n = 193)	81.8	7.8 (8.7)[1]	10.4
Parvi-recipient layer 4Cβ (n = 196)	81.9	6.1 (6.9)	12.2
Postsynaptic targets (layer 4C)			
PV-ir:Non-ir targets (n = 39:350)	10:90	8:92	10:90
PV-ir targets only (n = 39)	82	8	10
PV-ir targets contacted by asymmetric synapses only (n = 35)	91	9	

[1]Percentage value in parenthesis is the mean percentage of the asymmetric synaptic population only.
[2]Non-ir, non-immunoreactive.
[3]PV-ir, parvalbumin-immunoreactive.

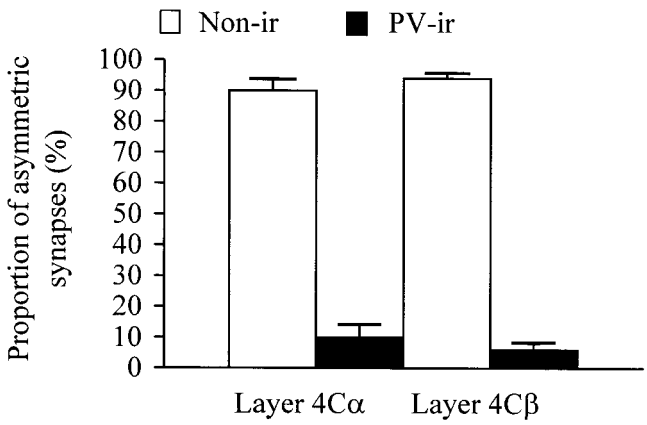

Fig. 6. Histogram showing the synaptic contribution of the dorsal lateral geniculate nucleus (dLGN) relay cells to the sublayers of layer 4C; layer 4Cα, and 4Cβ. Data are presented as means and S.E.M. values. For layer 4Cα, n = 193; for layer 4Cβ, n = 196. Non-ir, non-immunoreactive; PV-ir, parvalbumin-immunoreactive.

the estimates of the relative proportions of the two synapse types for each of the 3 monkeys was similar for both the magno-recipient and parvi-recipient layers 4Cα and 4Cβ (these figures are summarized in Table 1). A z-test indicated that there were no significant differences ($P < 0.05$) between monkeys within each synapse category for the same sublayer. Therefore, data from the three monkeys for each synapse category were pooled.

From the total of 389 identified synapses in layers 4Cα and 4Cβ, the majority of these synapses (89%) were asymmetric, the remainder being symmetric. The histogram in Figure 6 summarizes the principal findings with respect to the PV-ir of the presynaptic boutons. Most of the asymmetric synapses were formed by non-ir boutons. PV-ir boutons formed 8.7% of the asymmetric synapses in layer 4Cα (the magno-recipient layer) and 6.9% in layer 4Cβ (the parvi-recipient layer).

Targets of dLGN afferents

The 389 identified synapses were made with both PV-ir (n = 39) and unlabeled (n = 350) profiles (Figs. 4, 5, 7). Table 1 summarizes the distribution of the PV-ir and unlabeled synapses with their postsynaptic targets. Boutons that formed symmetrical synapses were not separated into PV-ir and unlabeled populations, because the number encountered in this study was too small for statistical analysis. The majority (90%) of synapses formed with the postsynaptic PV-ir profiles in layer 4 were asymmetric. Of this asymmetric population, PV-ir boutons formed only 9% of their synapses with PV-ir targets (Fig. 7B,C), the remainder being non-ir targets. The proportion of shafts and spines amongst the target structures was quite comparable between the two divisions of layer 4C. In layer 4Cα, 60% of the PV-ir boutons forming asymmetric synapses were formed with spines and 40% with dendritic shafts, whereas in layer 4Cβ, the comparable percentages were 58% and 41%, respectively.

DISCUSSION

The main aim of our anatomical study was to determine the contribution of the magno- and parvicellular layers of the dLGN to the population of asymmetric synapses in layer 4C of the macaque monkey. Previous estimates of the proportion of thalamocortical synapses in layer 4C of the primate ranged from 1.3% to 32%, depending on species, sublayer, and microzone within layer 4C (Garey and Powell, 1976; Tigges and Tigges, 1979; DeFelipe and Jones, 1991; Peters et al., 1994). There are many potential problems inherent in the estimates derived from conventional tracing studies, where differences in the uptake of a tracer, or the rate of degeneration of terminals, or the sampling methods used, can make large differences in the results. Such problems are also apparent in the cat cortical literature where the different methods used, of degeneration, anterograde transport of wheat germ agglutinin or radioactive proline, have produced estimates in the range of 5–30% (Garey and Powell, 1971; LeVay and Gilbert, 1976; LeVay, 1986). The proline result has given the highest value (LeVay and Gilbert, 1976), but is the least reliable, because proline is transported both anterogradely and retrogradely by both the dLGN afferents and layer 6 pyramidal cells that project to layer 4 (LeVay, 1986) and it leaks from the axons and boutons to produce additional transneuronal labeling (Peters and Payne, 1993). The methods used for sampling and counting synapses were also not specified in previous studies in the monkey (Garey and Powell, 1971; Tigges and Tigges, 1979; DeFelipe and Jones, 1991). Garey and Powell (1971) qualified their estimates by pointing out that they did not make corrections for possible differences in the rates of degeneration of the terminals arising from magno- or parvicellular layer, shrinkage, or phagocytosis, or the variation in the extent of the lesion between different layers of the dLGN.

Many of these difficulties are overcome in our approach, which followed the method of Jones and Hendry (1989) and DeFelipe and Jones (1991), in using the calcium-binding protein, parvalbumin, to identify the thalamocortical boutons in layer 4. Due to the high solubility of the protein, PV may be found throughout the cytosol (Baimbridge et al., 1992). Parvalbumin distributes within dendrites, and projecting axons of the thalamic relay cells as well as in the terminal boutons in the visual cortex (Jones and Hendry, 1989; DeFelipe and Jones, 1991). As seen previously in studies on macaque by Blümcke et al. (1991) and DeFelipe and Jones (1991), PV-ir cortical cells within striate cortex form

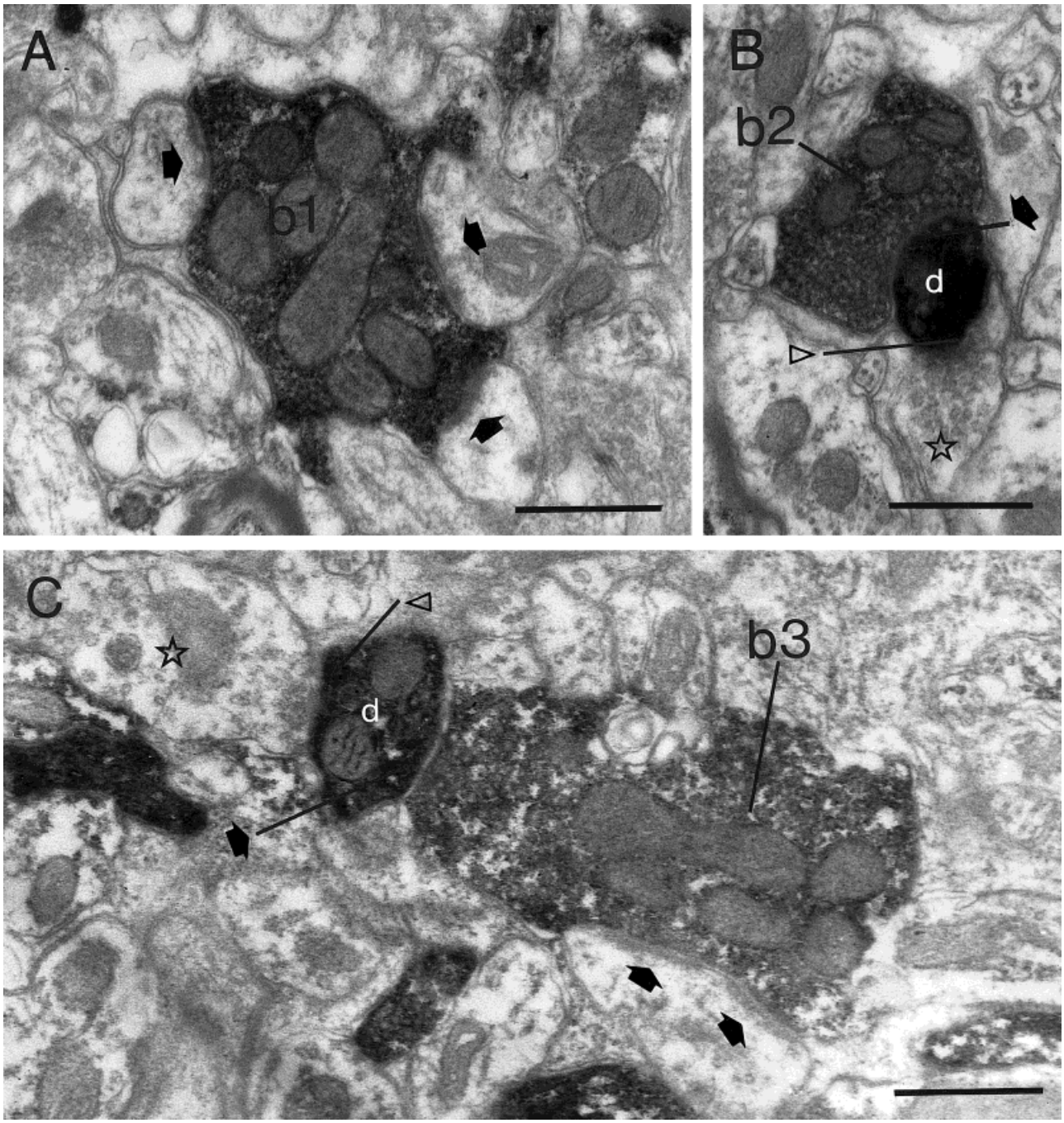

Fig. 7. Electron micrographs of parvalbumin-immunoreactive (PV-ir) boutons from putative dorsal lateral geniculate nucleus (dLGN) afferents found within layer 4C. The large PV-ir boutons (b1, b2) in **A** and **B** were located in the parvi-recipient layer 4Cβ, whereas b3 in **C** was located in the magno-recipient layer, 4Cα. A shows a putative dLGN bouton (b1) that forms more than one synapse (filled arrows). B and C show dLGN afferent boutons (b2, b3) that formed asymmetric synapses (filled arrows) with PV-ir and non-ir postsynaptic targets. In addition, the PV-ir targets (d, dendrite) formed synapses with non-ir boutons (star). In B, the synapse formed by the non-ir bouton (star) with the PV-ir postsynaptic target is asymmetric (open arrowhead). In C, the synapse formed by the non-ir bouton (star) is symmetric (open arrowhead). Scale bars = 0.5 μm.

symmetric (GABAergic) synapses (Figs. 4B,C, 5C,D). These were distinguishable from the PV-ir asymmetric synapses formed putatively by the terminal boutons from thalamic afferents within layer 4C of striate cortex (Figs. 4A, 5A,B). In addition, we used one of the nonbiased sampling procedures to count the synapses (Sterio, 1984).

An important consideration in using this method was whether all relay cells in the magno- and parvicellular

layers of the dLGN contain PV. The relay neurons that form part of the K pathway are located mainly in the interlaminar layers and project outside layer 4C (Hendry and Yoshioka, 1994). DeFelipe and Jones (1991) were uncertain whether all relay cells that project to layer 4C contain PV. Our analysis suggested that almost all neurons in dLGN layers 1–6 contain either PV and/or GABA, the exception being a small fraction of K neurons, which project outside layer 4C (Hendry and Yoshioka, 1994). The thalamic GABA-ir neurons are local circuit neurons and do not project to the cortex. Thus, we can be confident that there is not a significant population of non–PV-ir neurons that project from the dLGN to layer 4C. A further consideration is whether there are PV-ir projections to layer 4C from other nuclei. Although many neurons in nuclei outside the dLGN are PV-ir (Jones and Hendry, 1989), an extensive literature search failed to detect any likely candidates that project to layer 4C apart from the visual claustrum (Kennedy and Bullier, 1985; Perkel et al., 1986; Reynhout and Baizer, 1999). As in the cat (LeVay, 1986), the claustrum in the monkey probably projects to layer 4C, although this has not been specifically examined. In the cat, the dLGN terminals "probably greatly outnumber" the claustrocortical terminals in layer 4 (LeVay, 1986). For the purposes of our discussion, we have assumed the same applies in the monkey and that although there may be a minor contribution from claustrum, our estimates do reflect an upper limit on the possible proportion of dLGN synapses.

Assuming layer 4C is equally subdivided into 4Cα and 4Cβ (Blasdel and Fitzpatrick, 1984; Fitzpatrick et al., 1983; Livingstone and Hubel, 1984), we estimate that the thalamic contribution to the total excitatory input to layer 4C is 7.9%. This is subdivided into 8.7% of synapses in the magno-recipient layer 4Cα and 6.9% in the parvi-recipient layer 4Cβ. Compared with previous studies, our estimate of the dLGN contribution to layer 4C is in the range 5–10% obtained in degeneration studies in monkey (Garey and Powell, 1971; Winfield and Powell, 1983). This similarity is remarkable, given that we derived our data based on the stereological nonbiased physical disector method, which had not been developed at the time of the previous studies. This stereological method should give a more precise estimate (Sterio, 1984; Coggeshall and Lekan, 1996; West, 1999), because it allows all profiles of interest to have an equal chance of being sampled, and will not be influenced by shape, size, distribution of the profile of interest, or even section thickness of the tissue being sampled (Sterio, 1984; Coggeshall and Lekan, 1996, West, 1999). Moreover, the number of disectors taken ensured that we obtained an average value for the contribution, despite local inhomogenetities in density (DeFelipe and Jones, 1991). DeFelipe and Jones (1991) found patches of about 10–50 μm diameter in layer 4Cβ where PV-ir boutons formed 32% of the asymmetric synapses compared to only 9% outside the puncta. However, their preliminary quantitative analysis indicated that these puncta occur at low density, about 3–8 patches per 10,000 μm^2. From their data, we have calculated that the average proportion of PV-ir asymmetric synapses in 4Cβ is ~10.5%, which is surprisingly close to our estimate, given the approximations involved.

Several studies have suggested that the magnocellular and parvicellular axonal input to these layers could have approximately equal proportions of the thalamic synaptic input to its sublayer (Winfield et al., 1982; Freund et al., 1985). However estimates by Peters et al. (1994) indicated that the parvicellular dLGN afferents could form as much as 6 times more asymmetric synapses in layer 4Cβ than did the magnocellular input in layer 4Cα. From their estimates, between 3.7% and 8.7% of the asymmetric synapses arise from thalamic afferents in layer 4Cβ, but only between 1.3% and 1.9% in layer 4Cα. Their estimate was based on data from horseradish peroxidase (HRP)-filled axons reported by Blasdel and Lund (1983), and by Freund et al. (1989) who found that each magnocellular axon formed about 3,000 boutons, which is about double the number formed by parvicellular axons. Freund et al. (1989) examined 2 magnocellular axons, which formed 2.1 synapses per bouton compared to 1.8 for one parvicellular axon and 2.6 for another. A more representative sample was obtained by Winfield et al. (1982), who serially reconstructed single dLGN boutons, identified by the degeneration technique. Each parvicellular bouton formed 1.5 synapses on average, whereas each magnocellular bouton formed 2.5 synapses per bouton on average. There is a clear amplification of the magnocellular input to primary visual cortex, as was also found in the cat (Winfield and Powell, 1983; Freund et al., 1985).

A simple estimate of the number of synapses per layer 4C neuron provided by the magno- or parvicellular pathways can be derived from the data of Beaulieu et al. (1992). Their data indicates that an average of 2,138 asymmetric synapses are formed with each neuron in layer 4Cβ. From this and other sources, Peters et al. (1994) estimated that about 3.7–8.7% of the asymmetric synapses were provided by the parvicellular layers of the dLGN. This corresponds to 37–191 dLGN synapses per neuron for layer 4Cβ. Our estimate of 148 dLGN synapses per neuron (i.e., 6.9% of 2,138) lies within this range. Blasdel and Fitzpatrick (1984) calculated that these synapses would be contributed by 20–40 convergent dLGN afferents in 4Cβ.

In layer 4Cα, about 2,135 asymmetric synapses are formed with each neuron (Beaulieu et al., 1992; note that the density of neurons and synapses is lower in layer 4Cα than in 4Cβ). We estimated that 8.7% of these asymmetric synapses are provided by the magnocellular layers of the dLGN. This corresponds to 185 dLGN synapses per neuron. However, a very different estimate of 40 dLGN synapses per 4Cα neurons was obtained by Peters et al. (1994) on the basis of magnocellular arbor sizes (Blasdel and Lund, 1983; Freund et al., 1989) and the same cell and synapse density measurements of Beaulieu et al. (1992) that we have used here. We are unable to reconcile the fivefold discrepancy between our present results and the estimates of Peters et al. (1994). There are several areas of uncertainty that could affect their estimates, including the precise number of magnocellular relay cells and the number of synapses formed by each magnocellular axon. For our part, we cannot entirely rule out the possibility that there is an unidentified source of parvalbumin-positive boutons that form a large number of asymmetric synapses with layer 4Cα neurons. For reasons outlined above, the claustral projection to cortex, which probably is PV-positive, is likely to contribute few synapses to layer 4C. The major sources of asymmetric synapses in layer 4C, i.e., the local spiny stellate cells and the layer 6 pyramidal cells (Lund and Boothe, 1975; Saint Marie and

Peters, 1985; Anderson et al., 1993; Wiser and Callaway, 1996), do not contain parvalbumin.

Our finding of a similarity in numbers of dLGN synapses between the subdivisions of layer 4C is anticipated by the data of Winfield et al. (1982), who found that the magno- and parvicellular afferents contribute approximately equal numbers of synapses to their subdivisions of layer 4C. One thing that does emerge from all these calculations is that the dLGN magnocellular pathway cannot possibly contribute more than 5–10% of the synapses in layer 4Cα: there are simply too few magno-relay cells available even on the most favorable estimates of dLGN cell numbers (Ahmad and Spear, 1993; Malpeli et al., 1996) and boutons per terminal arbor (Blasdel and Lund, 1983; Freund et al., 1989).

Our new estimates of the contribution of the thalamic afferent synapses to single neurons in the subdivisions of layer 4C, raise again the puzzle of the striking difference between cat and monkey in respect of the physiological properties of the neurons that receive direct input from the dLGN. In the monkey the estimates of the proportion of different receptive field types in layer 4C varies between studies (Hubel and Wiesel, 1968; Bullier and Henry, 1980; Blasdel and Fitzpatrick, 1984; Hawken and Parker, 1984; Livingstone and Hubel, 1984; Leventhal et al, 1995), but all agree that neurons with nonoriented receptive fields, which occur only rarely in the cat layer 4 (Hubel and Wiesel, 1962), are found in significant numbers in the monkey, particularly in layer 4Cβ where many of the receptive fields resemble more those of parvicellular dLGN neurons. Our new estimates indicate that this physiological difference is not explained by large differences in the number of dLGN synapses in layer 4 between cat and monkey, because the numbers of thalamocortical synapses per neuron in the monkey are comparable to those of the cat. It is unlikely that there would be a quite different rule for the way in which the dLGN afferents map onto the dendritic trees of neurons in 4Cα vs. 4Cβ in monkey. This implies that other aspects of the circuitry must create the physiological differences between the sublaminae, the most obvious aspect being the great difference in the way that the layer 4 spiny stellate axons are distributed in layer 4. The layer 4Cα spiny stellates have extensive lateral projections, whereas the projections of the layer 4Cβ spiny stellates are vertical (Fisken et al., 1975; Fitzpatrick et al., 1985; Anderson et al., 1993). In this respect, the layer 4Cα spiny stellate in the monkey are much more like the layer 4 spiny stellates in the cat (Gilbert and Wiesel, 1979; Lund et al., 1979; Martin and Whitteridge, 1984; Peters and Payne, 1993) and are physiologically more alike. The differences in the lateral extent of spiny stellate axons in layer 4Cα compared to 4Cβ might thus contribute to the differences in the receptive field properties. Wörgötter and Eysel (1991) have shown, for example, that lateral connections in the cat visual cortex can contribute to the generation of orientation and direction selectivity.

Several studies have shown that layer 4C neurons receive inputs from sources other than the dLGN. Kisvarday et al. (1986) examined the dLGN synaptic input to smooth and spiny neurons in layer 4C by combining degeneration and Golgi-impregnation techniques. They found that thalamic synapses formed only a few percent of the total synapses formed with the dendrites of these neurons. Saint Marie and Peters (1985) provided evidence that other spiny stellate cells are a major source of input to each other. Although their study was based on a small sample of Golgi-stained cells, their reconstruction of the axonal projections of layer 4C spiny stellates indicated that their axons projected significantly within the layer of origin. Measurements of the profiles of the presynaptic boutons and the dimensions of the synapses indicated that their size overlapped almost completely with the size of the boutons formed by spiny stellate axons. The largest boutons, however, could not have originated from spiny stellate cells and they suggest that they probably originated from dLGN afferents.

Although these data point to the conclusion that the dLGN afferents and the spiny stellates between them provide the major excitatory input to layer 4, there is another major contribution to layer 4 from the layer 6 pyramidal cells, about which little is known at ultrastructural level in the monkey. In the cat, nearly half the asymmetric synapses formed with spiny stellate cells originate from layer 6 pyramidal cells (Ahmed et al., 1994, 1997). It is evident from Golgi studies, intracellular HRP, and bulk tracing studies that there is a substantial projection to layer 4 from layer 6 pyramidal cells in the macaque and that the axons have the same distinctive bottle-brush morphology seen in the cat (Lund and Boothe, 1975; Anderson et al., 1993; Wiser and Callaway, 1996). The synaptic targets of these projections have not been examined in the monkey, but in the cat the layer 6 pyramidal axons form synapses with the shafts of spiny and smooth neurons in layer 4 (McGuire et al., 1984; Ahmed et al., 1994, 1997). In the cat striate cortex, individual layer 6 pyramidal cells evoke small amplitude, facilitating excitatory postsynaptic potentials (E.P.S.P.s) in their layer 4 targets (Stratford et al., 1996), and similar physiology might apply in the monkey. Clearly, an explanation for the receptive field physiology of layer 4 in the monkey remains speculative. More quantitative and detailed studies, both at a physiological and anatomical level, need to be made of the synapses in layer 4 of the monkey if we are to unravel this intricate and interesting problem.

ACKNOWLEDGMENTS

This research was funded by a joint Swiss National Science Fund SPP grant to K.A.C.M. and Prof. R.J. Douglas.

LITERATURE CITED

Ahmad A, Spear PD. 1993. Effects of aging on the size, density and number of rhesus monkey lateral geniculate neurons. J Comp Neurol 334:631–643.

Ahmed B, Anderson JC, Douglas RJ, Martin KAC, Nelson JC. 1994. Polyneuronal innervation of spiny stellate neurons in cat visual cortex. J Comp Neurol 341:39–49.

Ahmed B, Anderson JC, Martin KAC, Nelson JC. 1997. Map of the synapses onto layer 4 basket cells of the primary visual cortex of the cat. J Comp Neurol 380:230–242.

Anderson J, Martin KAC, Whitteridge D. 1993. Form, function and intracortical projections of neurons in the striate cortex of the monkey *Maccacus nemestrinus.* Cerebral Cortex 3:412–420.

Baimbridge KG, Celio MR, Rogers JH. 1992. Calcium-binding proteins in the nervous system. Trends Neurosci 8:303–307.

Beaulieu C, Kisvarday Z, Somogyi P, Cynader M, Cowey A. 1992. Quantitative distribution of GABA-immunopositive and -immunonegative

neurons and synapses in the monkey striate cortex (area 17). Cerebral Cortex 2:295–309.

Blasdel GG, Fitzpatrick D. 1984. Physiological organization of layer 4 in macaque striate cortex. J Neurosci 4:880–895.

Blasdel GG, Lund JS. 1983. Termination of afferents axons in macaque striate cortex. J Neurosci 3:1389–1413.

Blümcke I, Hof PR, Morrison J, Celio M. 1990. Distribution of parvalbumin immunoreactivity in the visual cortex of old world monkeys and humans. J Comp Neurol 302:417–432.

Blümcke I, Hof PR, Morrison J, Celio M. 1991. Parvalbumin in the monkey striate cortex: a quantitative immunoelectron-microscopy study. Brain Res 554:237–143.

Bullier J, Henry GH. 1980. Ordinal position and afferent input of neurons in monkey striate cortex. J Comp Neurol 193:913–935.

Calverley PKS, Bedi KS, Jones DG. 1988. Estimation of the numerical density of synapses in rat neocortex. Comparison of the 'disector' with an 'unfolding' method. J Neurosci Methods 23:195–205.

Coggeshall RE. 1992. A consideration of neural counting methods. Trends Neurosci 15:9–13.

Coggeshall RE, Lekan HA. 1996. Methods for determining numbers of cells and synapses: a case for more uniform standards of review. J Comp Neurol 364:6–15.

DeFelipe J, Jones EG. 1991. Parvalbumin immunoreactivity reveals layer IV of monkey cerebral cortex as a mosaic of microzones of thalamic afferent terminations. Brain Res 562:39–47.

DeFelipe J, Hendry SHC, Jones EG. 1989. Visualisation of chandelier cell axons by parvalbumin immunoreactivity in monkey cerebral cortex. Proc Natl Acad Sci USA 89:2093–2097.

DeGroot DMG. 1988. Comparison of methods for the estimation of section thickness of ultrathin tissue sections. J Microsc 151:23–42.

Fisken RA, Garey LJ, Powell TPS. 1975. The intrinsic and commisural connections of area 17 of the visual cortex. Proc R Soc London (Biol) 272:487–536.

Fitzpatrick D, Itoh K, Diamond IT. 1983. The laminar organisation of the lateral geniculate body and the striate cortex in the squirrel monkey (*Samiri sciureus*). J Neurosci 3:673–702

Fitzpatrick D, Lund JS, Blasdel GG. 1985. Intrinsic connections of macaque striate cortex: afferent and efferent connections of lamina 4C. J Neurosci 5:3329–3349.

Freund TF, Martin KAC, Whitteridge D. 1985. Inervation of cat visual areas 17 and 18 by physiologically identified X- and Y- type thalamic afferents. I. Arborization patterns and quantitative distribution of postsynaptic elements. J Comp Neurol 242:263–274.

Freund TF, Martin KAC, Soltesz I, Somogyi P, Whitteridge D. 1989. Arborisation pattern and postsynaptic targets of physiologically identified thalamocortical afferents in striate cortex of the macaque monkey. J Comp Neurol 289:315–336.

Garey LJ, Powell TPS. 1971. An experimental study of the termination of the lateral geniculo-cortical pathway in the cat and monkey. Proc R Soc London (Biol) 179:21–40.

Geinisman Y, Gundersen HJG, Van Der Zee E, West MJ. 1996. Unbiased stereological estimation of the total number of synapses in a brain region. J Neurocytol 25:805–819.

Gilbert CD, Wiesel TN. 1979. Morphology and intracortical projections of functionally characterised neurons in the cat visual cortex. Nature 280:120–125.

Gundersen HJG. 1986. Stereology of arbitrary particles. A review of unbiased number and size estimators and the presentation of new ones, in memory of William R. Thompson. J Microsc 143:3–45.

Hawken MJ, Parker AJ. 1984. Contrast sensitivity and orientation selectivity in lamina IV of the striate cortex of old world monkeys. Exp Brain Res 54:367–372.

Hendry SHC, Calkins DJ. 1998. Neuronal chemistry and functional organization in the primate visual system. Trends Neurosci 21:344–349.

Hendry SHC, Yoshioka T. 1994. A neurochemically distinct third channel in the macaque dorsal lateral geniculate nucleus. Science 264:575–577.

Hendry SHC, Jones EG, Emson PC, Lawson DEM, Heizmann CW, Streit P. 1989. Two classes of cortical GABA neurons defined by differential calcium binding protein immunoreactivities. Exp Brain Res 475:156–159.

Hsu SM, Soban E. 1982. Colour modification of diaminobenzidine (DAB) precipitation by metallic ions and its application to double immunohistochemistry. J Histochem Cytochem 30:1079–1082.

Hubel DH, Wiesel TN. 1962. Receptive fields, binocular interaction and functional architecture in the cat's visual cortex. J Physiol 160:106–154.

Hubel DH, Wiesel TN. 1968. Receptive fields and functional architecture of monkey striate cortex. J Physiol 195:215–243.

Hunter A, Stewart MG. 1989. A quantitative analysis of the synaptic development of the lobus parolfactorius of the chick (*Gallus domesticus*). Exp Brain Res 78:425–434.

Jones EG, Hendry SHC. 1989. Differential calcium binding protein immunoreactivity distinguishes classes of relay neurones in monkey thalamic nuclei. Eur J Neurosci 1:222–246.

Kennedy H, Bullier J. 1985. A double labeling investigation of afferent connectivity of cortical areas V1 and V2 of the macaque monkey. J Neurosci 5: 2815–2830.

Kennedy H, Bullier J, Dehay C. 1985. Cytochrome oxidase activity in the striate cortex and lateral geniculate nucleus of the newborn and adult macaque monkey. Exp Brain Res 61:204–209.

Kisvarday ZF, Cowey A, Somogyi P. 1986. Synaptic relationships of a type of GABA-immunoreactive neuron (clutch cell), spiny stellate cells and lateral geniculate nucleus afferents in layer IVC of the monkey striate cortex. Neuroscience 3:741–761.

Lewis DA, Lund JS. 1990. Heterogeneity of chandelier neurons in monkey neocortex: corticotropin-releasing and parvalbumin-immunoreactive populations. J Comp Neurol 293:599–615.

LeVay S. 1986. Synaptic organisation of claustral and geniculate afferents to the visual cortex of the cat. J Neurosci 150:53–86.

LeVay S, Gilbert CD. 1976. Laminar patterns of geniculocortical projections in the cat. Brain Res 113:1–19.

Leventhal AG, Thompson KG, Liu D, Zhou Y, Ault SJ. 1995. Concomitant sensitivity to orientation, direction, and color of cells in layers 2, 3, 4 of monkey striate cortex. J Neurosci 15:1808–1818.

Livingstone MS, Hubel DH. 1984. Anatomy and physiology of a color system in the primate visual cortex. J Neurosci 4:309–356.

Lund JS, Boothe R. 1975. Interlaminar connections and pyramidal neuron organization in the visual cortex, area 17, of the macaque monkey. J Comp Neurol 159:305–334.

Lund JS, Hendry GH, MacQueen CL, Harvey AR. 1979. Anatomical organization of the visual cortex of the cat: a comparison with area 17 of the macaque monkey. J Comp Neurol 184:599–618.

Malpeli JG, Lee D, Baker FH. 1996. Laminar and retinotopic organization of the macaque lateral geniculate nucleus: magnocellular and parvocellular magnification functions. J Comp Neurol 375:363–377.

Martin KAC, Whitteridge D. 1984. Form, function and intracortical projections of spiny neurones in striate visual cortex of the cat. J Physiol 353:463–504.

McGuire BA, Hornung J-P, Gilbert CD, Wiesel TN. 1984. Patterns of synaptic input to layer 4 of cat striate cortex. J Neurosci 4:572–588.

Montero VM, Zempel J. 1986. The proportion and size of GABA-immunoreactive neurons in the magnocellular and parvocellular layers of the lateral geniculate nucleus of the rhesus monkey. Exp Brain Res 62:215–223.

Perkel DJ, Bullier J, Kennedy H. 1986. Topography of the afferent connectivity of area 17 in the macaque monkey: a double labelling study. J Comp Neurol 253:374–402.

Peters A, Payne BR. 1993. Numerical relationships between geniculocortical afferents and pyramidal cell modules in cat primary visual cortex. Cerebral Cortex 3:69–78.

Peters A, Sethares C, Harriman KM. 1990. Different kinds of axon terminals forming symmetric synapses with the cell bodies and initial axon segments of layer II/III pyramidal cells II. Synaptic junctions. J Neurocytol 19:584–600.

Peters A, Palay SL, Webster HDeF. 1991. The fine structure of the nervous system: neurons and their supporting cells, 3rd ed. Oxford: Oxford University Press.

Peters A, Payne BR, Budd J. 1994. A numerical analysis of the geniculocortical input to striate cortex in the monkey. Cerebral Cortex 4:215–229.

Reynhout K, Baizer JS. 1999. Immunoreactivity for calcium-binding proteins in the claustrum of the monkey. Anat Embryol 199:75–83.

Royet JP. 1991. Stereology: a method for analysing images. Prog Neurobiol 37:433–474.

Saint Marie RL, Peters A. 1985. The morphology and synaptic connections of spiny stellate neurons in monkey visual cortex (area 17): A Golgi-electron microscopic study. J Comp Neurol 233:213–235.

Small JD. 1968. Measurement of section thickness. Abstracts of the Fourth

European Regional Conference on Electron Microscopy (Rome) 1:609–610.

Sterio DC. 1984. The unbiased estimation of number and sizes of arbitrary particles using the disector. J Microsc 134:127–136.

Stratford KJ, Tarczy-Hornach K, Martin KAC, Bannister NJ, Jack JJB. 1996. Excitatory synaptic inputs to spiny stellate cells in cat visual cortex. Nature 382:258–261.

Tigges M, Tigges J. 1979. Types of degenerating geniculocortical axon terminals and their contribution to layer IV of area 17 in the squirrel monkey (*Saimiri*). Cell Tissue Res 196:471–486.

Van Brederode JFM, Mulligan KA, Hendrickson AE. 1990. Calcium-binding proteins as markers for subpopulations of GABAergic neurons in monkey striate cortex. J Comp Neurol 298:1–22.

Weibel ER. 1979. Stereological methods. Vol. 1. Practical methods for biological morphometry. Academic Press: New York

West M. 1999. Stereological methods for estimating the total number of neurons and synapses: issues of precision and bias. Trends Neurosci 22:51–61.

Winfield DA, TPS Powell. 1983. Laminar cell counts and geniculo-cortical boutons in area 17 of cat and monkey. Brain Res 277:223–229.

Winfield DA, Rivera-Dominguez M, Powell TPS. 1982. The termination of geniculocortical fibres in area 17 of the visual cortex in the macaque monkey. Brain Res 231:19–32.

Wiser AK, Callaway E. 1996. Contributions of individual layer 6 pyramidal neurons to local circuitry in macaque primary visual cortex. J Neurosci 16:2724–2739.

Wong-Riley M. 1979. Changes in the visual system of monocularly sutured or enucleated cats demonstrable with cytochrome oxidase histochemistry. Brain Res 171:11–28.

Wörgötter F, Eysel UT. 1991. Topographical aspects of intracortical excitation and inhibition contributing to orientation specificity in area 17 of the cat visual cortex. Eur J Neurosci 3:1232–1244.